12

Feedback Amplifier Configurations

John Choma, Jr.
University of Southern California

12.1 Introduction

Four basic types of single-loop feedback amplifiers are available: the **series-shunt**, **shunt-series**, **shunt-shunt**, and **series-series architectures** [1]. Each of these cells is capable of a significant reduction of the dependence of forward transfer characteristics on the ill-defined or ill-controlled parameters implicit to the open-loop gain; but none of these architectures can simultaneously offer controlled driving-point input and output impedances. Such additional control is afforded only by dual global loops comprised of series and/or shunt feedback signal paths appended to an open-loop amplifier [2], [3]. Only two types of global dual-loop feedback architectures are used: the **series-series/shunt-shunt feedback amplifier** and the **series-shunt/shunt-series feedback amplifier**.

Although only bipolar technology is exploited in the analysis of the aforementioned four single-loop and two dual-loop feedback cells, all disclosures are generally applicable to metaloxide-silicon (MOS), heterostructure bipolar transistor (HBT), and III–V compound metal-semiconductor field-effect transistor (MESFET) technologies. All analytical results derive from an application of a hybrid, signal flow/two-port parameter analytical tack. Because the thought processes underlying this technical approach apply to all feedback circuits, the subject analytical procedure is developed in detail for only the series-shunt feedback amplifier.

12.2 Series-Shunt Feedback Amplifier

Circuit Modeling and Analysis

Figure 12.1(a) depicts the **ac schematic diagram** (a circuit diagram divorced of biasing details) of a series-shunt feedback amplifier. In this circuit, the output voltage V_O, which is established in response to a single source represented by the Thévenin voltage V_{ST}, and the Thévenin resistance, R_{ST}, is sampled by

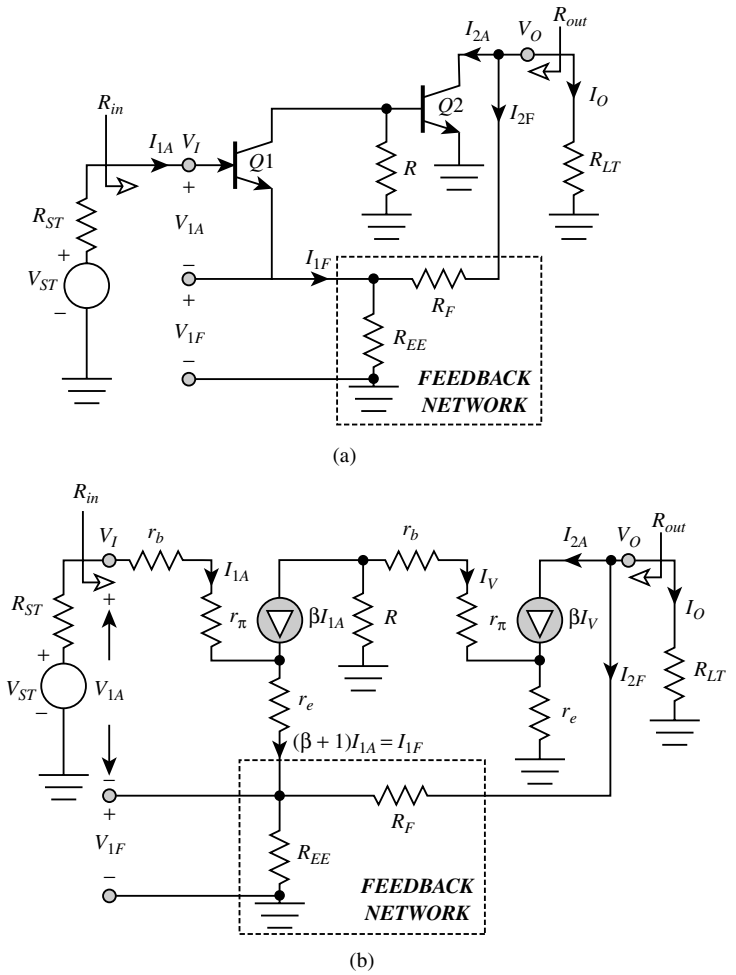

FIGURE 12.1 (a) The ac schematic diagram of a bipolar series-shunt feedback amplifier. (b) Low-frequency small-signal equivalent circuit of the feedback amplifier.

the feedback network composed of the resistances, R_{EE} and R_F. The sampled voltage is fed back in such a way that the closed-loop input voltage, V_I, is the sum of the voltage, V_{1A}, across the input port of the amplifier and the voltage V_{1F}, developed across R_{EE} in the feedback subcircuit. Because $V_I = V_{1A} + V_{1F}$, the output port of the feedback configuration can be viewed as connected in series with the amplifier input port. On the other hand, output voltage sampling constrains the net load current, I_O, to be the algebraic sum of the amplifier output port current, I_{2A}, and the feedback network input current, I_{2F}. Accordingly, the output topology is indicative of a shunt connection between the feedback subcircuit and the amplifier output port. The fact that voltage is fed back to a voltage-driven input port renders the driving point input resistance, R_{in}, of the closed-loop amplifier large, whereas the driving-point output resistance, R_{out}, seen by the terminating load resistance, R_{LT}, is small. The resultant closed-loop amplifier is therefore best suited for voltage amplification, in the sense that the closed-loop voltage gain, V_O/V_{ST}, can be made approximately independent of source and load resistances. For large loop gain, this voltage transfer function is also nominally independent of transistor parameters.

Assuming that transistors $Q1$ and $Q2$ are identical devices that are biased identically, Figure 12.1(b) is the applicable low-frequency equivalent circuit. This equivalent circuit exploits the hybrid-π model [4] of a bipolar junction transistor, subject to the proviso that the forward Early resistance [5] used to emulate base conductivity modulation is sufficiently large to warrant its neglect. Because an infinitely

large forward Early resistance places the internal collector resistance (not shown in the figure) of a bipolar junction transistor in series with the current controlled current source, this collector resistance can be ignored as well.

The equivalent circuit of Figure 12.1(b) can be reduced to a manageable topology by noting that the ratio of the signal current, I_V, flowing into the base of transistor $Q2$ to the signal current, I_{1A}, flowing into the base of transistor $Q1$ is

$$\frac{I_V}{I_{1A}} \triangleq -K_\beta = -\frac{\beta R}{R + r_b + r_\pi + (\beta + 1) r_e} = -\frac{\alpha R}{r_{ib} + (1 - \alpha) R} \tag{12.1}$$

where

$$\alpha = \frac{\beta}{\beta + 1} \tag{12.2}$$

is the small-signal, short-circuit common base current gain, and

$$r_{ib} = r_e + \frac{r_\pi + r_b}{\beta + 1} \tag{12.3}$$

symbolizes the short-circuit input resistance of a common base amplifier. It follows that the current source βI_v in Figure 12.1(b) can be replaced by the equivalent current $(-\beta K_\beta I_{1A})$.

A second reduction of the equivalent circuit in Figure 12.1(b) results when the feedback subcircuit is replaced by a model that reflects the *h*-parameter relationships

$$\begin{bmatrix} V_{1F} \\ I_{2F} \end{bmatrix} = \begin{bmatrix} h_{if} & h_{rf} \\ h_{ff} & h_{of} \end{bmatrix} \begin{bmatrix} I_{1F} \\ V_o \end{bmatrix} \tag{12.4}$$

where $V_{1F}(V_O)$ represents the signal voltage developed across the output (input) port of the feedback subcircuit and $I_{1F}(I_{2F})$ symbolizes the corresponding current flowing into the feedback output (input) port. Although any homogeneous set of two-port parameters can be used to model the feedback subcircuit, *h* parameters are the most convenient selection herewith. In particular, the feedback amplifier undergoing study is a series-shunt configuration. The *h*-parameter equivalent circuit represents its input port as a Thévenin circuit and its input port as a Norton configuration, therefore, the *h*-parameter equivalent circuit is likewise a series-shunt structure.

For the feedback network at hand, which is redrawn for convenience in Figure 12.2(a), the *h*-parameter equivalent circuit is as depicted in Figure 12.2(b). The latter diagram exploits the facts that the short-circuit input resistance h_{if} is a parallel combination of the resistance R_{EE} and R_F, and the open-circuit output conductance h_{of}, is $1/(R_{\text{EE}} + R_F)$. The open-circuit reverse voltage gain h_{rf} is

$$h_{rf} = \frac{R_{\text{EE}}}{R_{\text{EE}} + R_F} \tag{12.5}$$

while the short-circuit forward current gain h_{ff} is

$$h_{ff} = \frac{R_{\text{EE}}}{R_{\text{EE}} + R_F} = -h_{rf} \tag{12.6}$$

Figure 12.2(c) modifies the equivalent circuit in Figure 12.2(b) in accordance with the following two arguments. First, h_{rf} in (12.5) is recognized as the fraction of the feedback subcircuit input signal that is

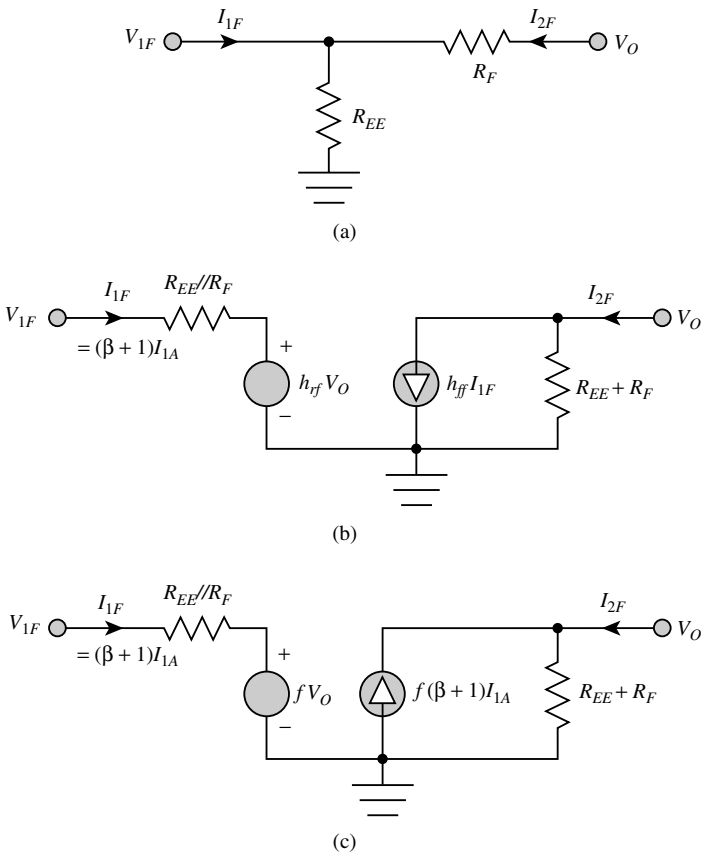

FIGURE 12.2 (a) The feedback subcircuit in the series-shunt feedback amplifier of Figure 12.1(a). (b) The *h*-parameter equivalent circuit of the feedback subcircuit. (c) Alternative form of the *h*-parameter equivalent circuit.

fed back as a component of the feedback subcircuit output voltage, V_{1F}. But this subcircuit input voltage is identical to the closed-loop amplifier output signal V_O. Moreover, V_{1F} superimposes with the Thévenin input signal applied to the feedback amplifier to establish the amplifier input port voltage, V_{1A}. It follows that h_{rf} is logically referenced as a feedback factor, say f, of the amplifier under consideration; that is,

$$h_{rf} = \frac{R_{\text{EE}}}{R_{\text{EE}} + R_F} \triangleq f \tag{12.7}$$

and by (12.6),

$$h_{ff} = -\frac{R_{\text{EE}}}{R_{\text{EE}} + R_F} = -f \tag{12.8}$$

Second, the feedback subcircuit output current, I_{1F}, is, as indicated in Figure 12.1(b), the signal current, $(\beta + 1)I_{1A}$. Thus, in the model of Figure 12.2(b),

$$h_{ff}I_{1F} = -f(\beta + 1)I_{1A} \tag{12.9}$$

If the model in Figure 12.2(c) is used to replace the feedback network in Figure 12.1(b) the equivalent circuit of the series-shunt feedback amplifier becomes the alternative structure offered in Figure 12.3. In

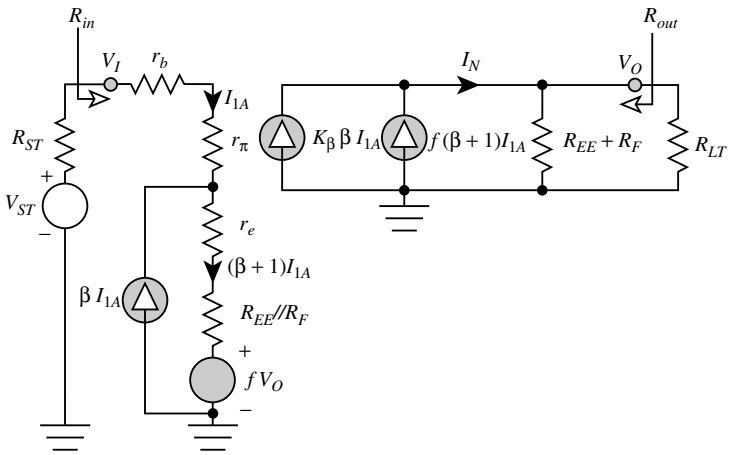

FIGURE 12.3 Modified small-signal model of the series-shunt feedback amplifier.

arriving at this model, care has been exercised to ensure that the current flowing through the emitter of transistor $Q1$ is $(\beta + 1)I_{1A}$. It is important to note that the modified equivalent circuit delivers transfer and driving point impedance characteristics that are identical to those implicit to the equivalent circuit of Figure 12.1(b). In particular, the traditional analytical approach to analyzing a series-shunt feedback amplifier tacitly presumes the satisfaction of the Brune condition [6] to formulate a composite structure where the *h*-parameter matrix is the sum of the respective *h*-parameter matrices for the open-loop and feedback circuits. In contrast, the model of Figure 12.3 derives from Figure 12.1(b) without invoking the Brune requirement, which is often not satisfied. It merely exploits the substitution theorem; that is, the feedback network in Figure 12.1(b) is substituted by its *h*-parameter representation.

In addition to modeling accuracy, the equivalent circuit in Figure 12.3 boasts at least three other advantages. The first is an illumination of the vehicle by which feedback is implemented in the series-shunt configuration. This vehicle is the voltage controlled voltage source, $f\,V_O$, which feeds back a fraction of the output signal to produce a branch voltage that algebraically superimposes with, and thus modifies, the applied source voltage effectively seen by the input port of the open-loop amplifier. Thus, with $f = 0$, no feedback is evidenced, and the model at hand emulates an open-loop configuration. But even with $f = 0$, the transfer and driving-point impedance characteristics of the resultant open-loop circuit are functionally dependent on the feedback elements, R_{EE} and R_F, because appending the feedback network to the open-loop amplifier incurs additional impedance loads at both the input and the output ports of the amplifier.

The second advantage of the subject model is its revelation of the magnitude and nature of feed-forward through the closed loop. In particular, note that the signal current, I_N, driven into the effective load resistance comprised of the parallel combination of $(R_{EE} + R_F)$ and R_{LT}, is the sum of two current components. One of these currents, $\beta K_\beta I_{1A}$, materializes from the transfer properties of the two transistors utilized in the amplifier. The other current, $f\,(\beta + 1)I_{1A}$, is the feed-forward current resulting from the bilateral nature of the passive feedback network. In general, negligible feed-forward through the feedback subcircuit is advantageous, particularly in high-frequency signal-processing applications. To this end, the model in Figure 12.3 suggests the design requirement,

$$f \ll \alpha K_\beta \tag{12.10}$$

When the resistance, R, in Figure 12.1(a) is the resistance associated with the output port of a PNP current source used to supply biasing current to the collector of transistor $Q1$ and the base of transistor $Q2$, K_β approaches β, and (12.10) is easily satisfied; however, PNP current sources are undesirable in broadband low-noise amplifiers. In these applications, the requisite biasing current must be supplied by

a passive resistance, R, connected between the positive supply voltage and the junction of the $Q1$ collector and the $Q2$ base. Unfortunately, the corresponding value of K_β can be considerably smaller than β, with the result that (12.10) may be difficult to satisfy. Circumvention schemes for this situation are addressed later.

A third attribute of the model in Figure 12.3 is its disposition to an application of signal flow theory. For example, with the feedback factor f selected as the reference parameter for signal flow analysis, the open-loop voltage gain $G_{vo}(R_{ST}, R_{LT})$, of the series-shunt feedback amplifier is computed by setting f to zero. Assuming that (12.10) is satisfied, circuit analysis reveals this gain as

$$G_{vo}\left(R_{ST}, R_{LT}\right) = \alpha K_\beta \left[\frac{\left(R_{EE} + R_F\right) \| R_{LT}}{r_{ib} + \left(1-\alpha\right) R_{ST} + \left(R_{EE} \| R_F\right)} \right] \tag{12.11}$$

The corresponding input and output driving point resistances, R_{ino} and R_{outo}, respectively, are

$$R_{ino} = r_B + r_\pi + \left(\beta + 1\right)\left(r_E + R_{EE} \| R_F\right) \tag{12.12}$$

and

$$R_{outo} = R_{EE} + R_F \tag{12.13}$$

It follows that the closed-loop gain $G_v\left(R_{ST}, R_{LT}\right)$ of the series-shunt feedback amplifier is

$$G_v\left(R_{ST}, R_{LT}\right) = \frac{G_{vo}\left(R_{ST}, R_{LT}\right)}{1 + T} \tag{12.14}$$

where the loop gain T is

$$\begin{aligned} T = f G_{vo}\left(R_{ST}, R_{LT}\right) &= \left(\frac{R_{EE}}{R_{EE} + R_F} \right) G_{vo}\left(R_{ST}, R_{LT}\right) \\ &= \alpha K_\beta \left(\frac{R_{EE}}{R_{EE} + R_F + R_{LT}} \right) \left[\frac{R_{LT}}{r_{ib} + \left(1-\alpha\right) R_{ST} + \left(R_{EE} \| R_F\right)} \right] \end{aligned} \tag{12.15}$$

For $T \gg 1$, which mandates a sufficiently large K_β in (12.11), the closed-loop gain collapses to

$$G_v\left(R_{ST}, R_{LT}\right) \approx \frac{1}{f} = 1 + \frac{R_F}{R_{EE}} \tag{12.16}$$

which is independent of active element parameters. Moreover, to the extent that $T \gg 1$ the series-shunt feedback amplifier behaves as an ideal voltage controlled voltage source in the sense that its closed-loop voltage gain is independent of source and load terminations. The fact that the series-shut feedback network behaves approximately as an ideal voltage amplifier implies that its closed-loop driving point input resistance is very large and its closed-loop driving point output resistance is very small. These facts are confirmed analytically by noting that

$$\begin{aligned} R_{in} = R_{ino}\left[1 + f G_{vo}\left(0, R_L\right)\right] &\approx f R_{ino} G_{vo}\left(0, R_L\right) \\ &= \beta K_\beta \left(\frac{R_{EE}}{R_{EE} + R_F + R_{LT}} \right) R_{LT} \end{aligned} \tag{12.17}$$

and

$$R_{\text{out}} = \frac{R_{\text{outo}}}{1 + f G_{vo}\left(R_S, \infty\right)} \approx \frac{R_{\text{outo}}}{f G_{vo}\left(R_S, \infty\right)} = \left(1 + \frac{R_F}{R_{\text{EE}}}\right)\left[\frac{r_{ib} + (1-\alpha)R_{\text{ST}} + R_{\text{EE}} \| R_F}{\alpha K_\beta}\right] \tag{12.18}$$

To the extent that the interstage biasing resistance, R, is sufficiently large to allow K_β to approach β, observe that R_{in} in (12.17) is nominally proportional to β^2, while R_{out} in (12.18) is inversely proportional to β.

Feed-Forward Compensation

When practical design restrictions render the satisfaction of (12.10) difficult, feed-forward problems can be circumvented by inserting an emitter follower between the output port of transistor $Q2$ in the circuit diagram of Figure 12.1(a) and the node to which the load termination and the input terminal of the feedback subcircuit are incident [2]. The resultant circuit diagram, inclusive now of simple biasing subcircuits, is shown in Figure 12.4. The buffer transistor $Q3$ increases the original short-circuit forward current gain, $K_\beta\beta$, of the open-loop amplifier by a factor approaching $(\beta + 1)$, while not altering the feed-forward factor implied by the feedback network in Figure 12.1(a). In effect, K_β is increased by a factor of almost $(\beta + 1)$, thereby making (12.10) easy to satisfy. Because of the inherently low output resistance of an emitter follower, the buffer also reduces the driving-point output resistance achievable by the original configuration.

The foregoing contentions can be confirmed through an analysis of the small-signal model for the modified amplifier in Figure 12.4. Such an analysis is expedited by noting that the circuit to the left of the current controlled current source, $K_\beta\beta I_{1A}$, in Figure 12.3 remains applicable. For zero feedback, it follows that the small-signal current I_{1A} flowing into the base of transistor $Q1$ derives from

$$\left.\frac{I_{1A}}{V_{\text{ST}}}\right|_{f=0} = \frac{1-\alpha}{r_{ib} + (1-\alpha)R_{\text{ST}} + \left(R_{\text{EE}} \| R_F\right)} \tag{12.19}$$

The pertinent small-signal model for the buffered series-shunt feedback amplifier is resultantly the configuration offered in Figure 12.5.

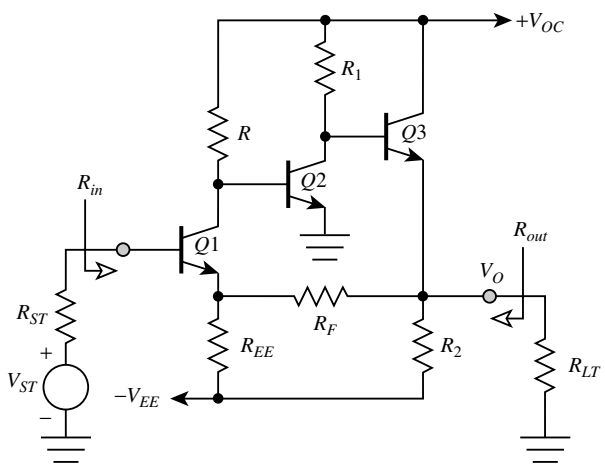

FIGURE 12.4 A series-shunt feedback amplifier that incorporates an emitter follower output stage to reduce the effects of feed-forward through the feedback network.

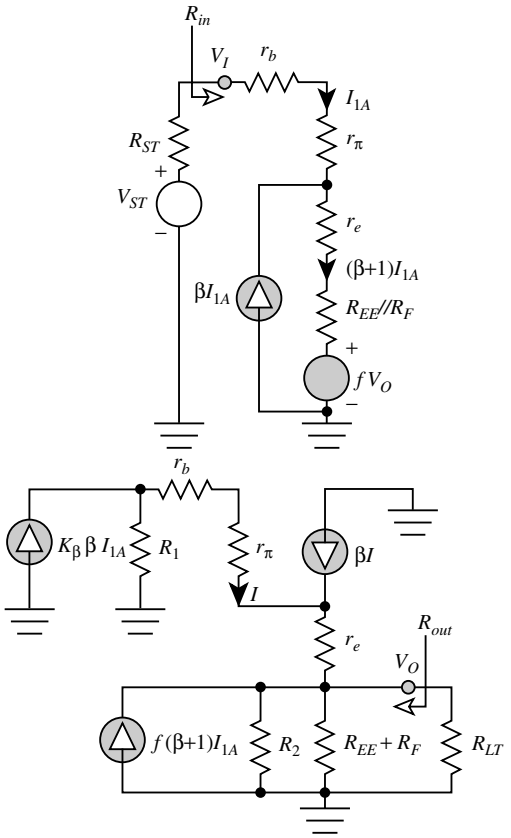

FIGURE 12.5 Small-signal model of the buffered series-shunt feedback amplifier.

Letting

$$R' = R_2 \left\| \left(R_{\mathrm{EE}} + R_F\right) \right\| R_{\mathrm{LT}} \tag{12.20}$$

an analysis of the structure in Figure 12.5 reveals

$$\frac{V_O}{I_{1A}} = (\beta+1)\left[\frac{R'}{R' + r_{ib} + (1-\alpha)R_1}\right]\left\{\alpha K_\beta R_1 + f\left[r_{ib} + (1-\alpha)R_1\right]\right\} \tag{12.21}$$

which suggests negligible feed-forward for

$$f \ll \frac{\alpha K_\beta R_1}{r_{ib} + (1-\alpha)R_1} \tag{12.22}$$

Note that for large R_1, (12.22) implies the requirement $f \ll \beta K_\beta$, which is easier to satisfy than is (12.10). Assuming the validity of (12.22), (12.21), and (12.19) deliver an open-loop voltage gain,. $G_{vo}(R_{\mathrm{ST}}, R_{\mathrm{LT}})$, of

$$G_{vo}\left(R_{\mathrm{ST}}, R_{\mathrm{LT}}\right) = \alpha K_\beta \left[\frac{R'}{r_{ib} + (1-\alpha)R_{\mathrm{ST}} + R_{\mathrm{EE}} \| R_F}\right]\left[\frac{R_1}{R' + r_{ib} + (1-\alpha)R_1}\right] \tag{12.23}$$

Recalling (12.1), which demonstrates that K_β approaches β for large R, (12.23) suggests an open-loop gain that is nominally proportional to β^2 if R_1 is also large.

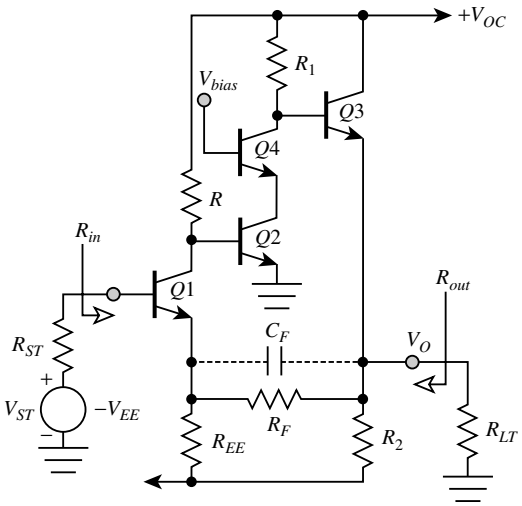

FIGURE 12.6 Buffered series-shunt feedback amplifier with common base cascode compensation of the common emitter amplifier formed by transistor $Q2$. A feedback zero is introduced by the capacitance C_F to achieve acceptable closed-loop damping.

Using the concepts evoked by (12.17) and (12.18), the driving-point input and output impedances can now be determined. In a typical realization of the buffered series-shunt feedback amplifier, the resistance, R_2, in Figure 12.4 is very large because it is manifested as the output resistance of a common base current sink that is employed to stabilize the operating point of transistor $Q3$. For this situation, and assuming the resistance R_1 is large, the resultant driving-point input resistance is larger than its predecessor input resistance by a factor of approximately $(\beta + 1)$. Similarly, it is easy to show that for large R_1 and large R_2, the driving-point output resistance is smaller than that predicted by (12.18) by a factor approaching $(\beta + 1)$.

Although the emitter follower output stage in Figure 12.4 all but eliminates feed-forward signal transmission through the feedback network and increases both the driving point input resistance and output conductance, a potential bandwidth penalty is paid by its incorporation into the basic series-shunt feedback cell. The fundamental problem is that if R_1 is too large, potentially significant Miller multiplication of the base-collector transition capactiance of transistor $Q2$ materializes. The resultant capacitive loading at the collector of transistor $Q1$ is exacerbated by large R, which may produce a dominant pole at a frequency that is too low to satisfy closed-loop bandwidth requirements. The bandwidth problem may be mitigated by coupling resistance R_1 to the collector of $Q2$ through a common base cascode. This stage appears as transistor $Q4$ in Figure 12.6.

Unfortunately, the use of the common base cascode indicated in Figure 12.6 may produce an open-loop amplifier with transfer characteristics that do not emulate a dominant pole response. In other words, the frequency of the compensated pole established by capacitive loading at the collector of transistor $Q1$ may be comparable to the frequencies of poles established elsewhere in the circuit, and particularly at the base node of transistor $Q1$. In this event, frequency compensation aimed toward achieving acceptable closed-loop damping can be implemented by replacing the feedback resistor R_F with the parallel combination of R_F and a feedback capacitance, say C_F, as indicated by the dashed branch in Figure 12.6. The resultant frequency-domain feedback factor $f(s)$ is

$$f(s) = f\left[\frac{1+\frac{s}{z}}{1+\frac{fs}{z}}\right] \tag{12.24}$$

where f is the feedback factor given by (12.7) and z is the frequency of the introduced compensating zero, is

$$z = \frac{1}{R_F C_F} \tag{12.25}$$

The pole in (12.24) is inconsequential if the closed-loop amplifier bandwidth B_{cl} satisfies the restriction, $f B_{cl} R_F C_F = B_{cl}(R_{EE} \| R_F) C_F \ll 1$.

12.3 Shunt-Series Feedback Amplifier

Although the series-shunt circuit functions as a voltage amplifier, the shunt-series configuration (see the ac schematic diagram depicted in Figure 12.7(a)) is best suited as a current amplifier. In the subject circuit, the $Q2$ emitter current, which is a factor of $(1/\alpha)$ of the output signal current, I_O, is sampled by the feedback network formed of the resistances, R_{EE} and R_F. The sampled current is fed back as a current in shunt with the amplifier input port. Because output current is fed back as a current to a current-

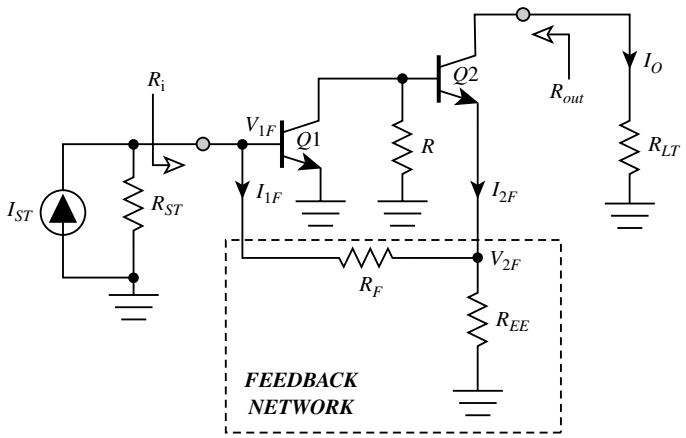

(a)

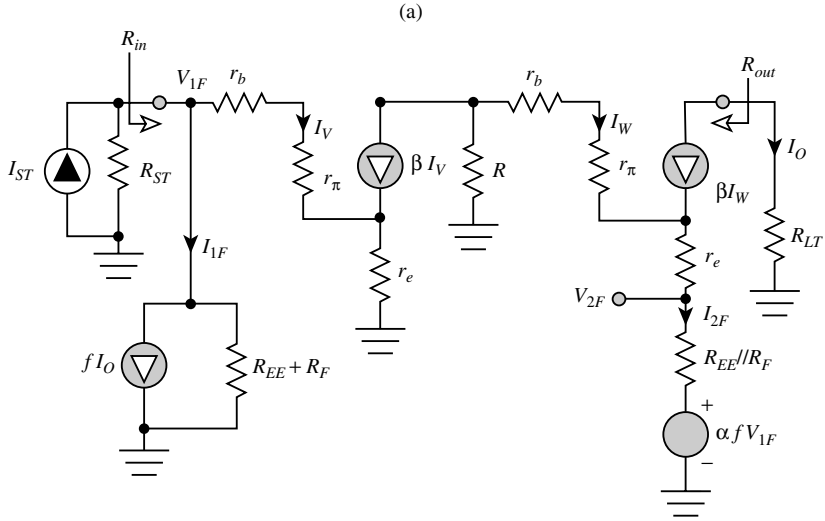

(b)

FIGURE 12.7 (a) AC schematic diagram of a bipolar shunt-series feedback amplifier. (b) Low-frequency small-signal equivalent circuit of the feedback amplifier.

driven input port, the resultant driving point output resistance is large, and the driving-point input resistance is small. These characteristics allow for a closed-loop current gain, $G_I(R_{ST}, R_{LT}) = I_o/I_{ST}$, that is relatively independent of source and load resistances and insensitive to transistor parameters.

In the series-shunt amplifier, *h* parameters were selected to model the feedback network because the topology of an *h*-parameter equivalent circuit is, similar to the amplifier in which the feedback network is embedded, a series shunt, or Thévenin–Norton, topology, In analogous train of thought compels the use of *g*-parameters to represent the feedback network in Figure 12.7(a). With reference to the branch variables defined in the schematic diagram,

$$\begin{bmatrix} I_{1F} \\ V_{2F} \end{bmatrix} = \begin{bmatrix} \dfrac{1}{R_{EE}+R_F} & -\dfrac{R_{EE}}{R_{EE}+R_F} \\ \dfrac{R_{EE}}{R_{EE}+R_F} & R_{EE}\|R_F \end{bmatrix} \begin{bmatrix} V_{1F} \\ I_{2F} \end{bmatrix} \tag{12.26}$$

Noting that the feedback network current, I_{2F}, relates to the amplifier output current, I_O, in accordance with

$$I_{2F} = -\frac{I_O}{\alpha} \tag{12.27}$$

and letting the feedback factor, *f*, be

$$f = \frac{1}{\alpha}\left(\frac{R_{EE}}{R_{EE}+R_F}\right) \tag{12.28}$$

the small-signal equivalent circuit of shunt-series feedback amplifier becomes the network diagrammed in Figure 12.7(b). Note that the voltage controlled voltage source, $\alpha f V_{1F}$, models the feed-forward transfer mechanism of the feedback network, where the controlling voltage, V_{1F}, is

$$V_{1F} = \left[r_b + r_\pi + (\beta+1)r_c\right]I_V = (\beta+1)r_{ib}I_V \tag{12.29}$$

An analysis of the model in Figure 12.7(b) confirms that the second-stage, signal-base current I_w relates to the first-stage, signal-base current I_v as

$$\frac{I_W}{I_V} = -\frac{\alpha\left(R+fr_{ib}\right)}{r_{ib}+R_{EE}\|R_F+(1-\alpha)R} \tag{12.30}$$

For

$$f \ll \frac{R}{r_{ib}} \tag{12.31}$$

which offsets feed-forward effects,

$$\frac{I_W}{I_V} \approx -\frac{\alpha R}{r_{ib}+R_{EE}\|R_F+(1-\alpha)R} \triangleq -K_r \tag{12.32}$$

Observe that the constant K_r tends toward β for large *R*, as can be verified by an inspection of Figure 12.7(b).

Using (12.32), the open-loop current gain, found by setting f to zero, is

$$G_{\mathrm{IO}}\left(R_{\mathrm{ST}},R_{\mathrm{LT}}\right)=\left.\frac{I_O}{I_{\mathrm{ST}}}\right|_{f=0}=\alpha K_r\left\{\frac{R_{\mathrm{ST}}\left\|\left(R_{\mathrm{EE}}+R_F\right)\right.}{r_{ib}+\left(1-\alpha\right)\left[R_{\mathrm{ST}}\left\|\left(R_{\mathrm{EE}}+R_F\right)\right.\right]}\right\} \tag{12.33}$$

and, recalling (12.28), the loop gain T is

$$\begin{aligned}T=fG_{\mathrm{IO}}\left(R_{\mathrm{ST}},R_{\mathrm{LT}}\right)&=\frac{1}{\alpha}\left(\frac{R_{\mathrm{EE}}}{R_{\mathrm{EE}}+R_F}\right)G_{\mathrm{IO}}\left(R_{\mathrm{ST}},R_{\mathrm{LT}}\right)\\&=K_r\left(\frac{R_{\mathrm{EE}}}{R_{\mathrm{EE}}+R_F+R_{\mathrm{ST}}}\right)\left\{\frac{R_{\mathrm{ST}}}{r_{ib}+\left(1-\alpha\right)\left[R_{\mathrm{ST}}\left\|\left(R_{\mathrm{EE}}+R_F\right)\right.\right]}\right\}\end{aligned} \tag{12.34}$$

By inspection of the model in Figure 12.7(b), the open-loop input resistance, R_{ino}, is

$$R_{\mathrm{ino}}=\left(R_{\mathrm{EE}}+R_F\right)\left\|\left[\left(\beta+1\right)r_{ib}\right]\right. \tag{12.35}$$

and, within the context of an infinitely large Early resistance, the open-loop output resistance, R_{outo}, is infinitely large.

The closed-loop current gain of the shunt-series feedback amplifier is now found to be

$$G_{\mathrm{I}}\left(R_{\mathrm{ST}},R_{\mathrm{LT}}\right)=\frac{G_{\mathrm{IO}}\left(R_{\mathrm{ST}},R_{\mathrm{LT}}\right)}{1+T}\approx\alpha\left(1+\frac{R_F}{R_{\mathrm{EE}}}\right) \tag{12.36}$$

where the indicated approximation exploits the presumption that the loop gain T is much larger than one. As a result of the large loop-gain assumption, note that the closed-loop gain is independent of the source and load resistances and is invulnerable to uncertainties and perturbations in transistor parameters. The closed-loop output resistance, which exceeds its open-loop counterpart, remains infinitely large. Finally, the closed-loop driving point input resistance of the shunt-series amplifier is

$$R_{\mathrm{in}}=\frac{R_{\mathrm{ino}}}{1+fG_{\mathrm{IO}}\left(\infty,R_{\mathrm{LT}}\right)}\approx\left(1+\frac{R_F}{R_{\mathrm{EE}}}\right)\frac{r_{ib}}{K_r} \tag{12.37}$$

12.4 Shunt-Shunt Feedback Amplifier

Circuit Modeling and Analysis

The ac schematic diagram of the third type of single-loop feedback amplifier, the shunt-shunt triple, is drawn in Figure 12.8(a). A cascade interconnection of three transistors $Q1$, $Q2$, and $Q3$, forms the open loop, while the feedback subcircuit is the single resistance, R_F. This resistance samples the output voltage, V_O, as a current fed back to the input port. Output voltage is fed back as a current to a current-driven input port, so both the driving point input and output resistances are very small. Accordingly, the circuit operates best as a transresistance amplifier in that its closed-loop transresistance, $R_M\left(R_{\mathrm{ST}},R_{\mathrm{LT}}\right)=V_O/I_{\mathrm{ST}}$, is nominally invariant with source resistance, load resistance, and transistor parameters.

The shunt-shunt nature of the subject amplifier suggests the propriety of y-parameter modeling of the feedback network. For the electrical variables indicated in Figure 12.8(a),

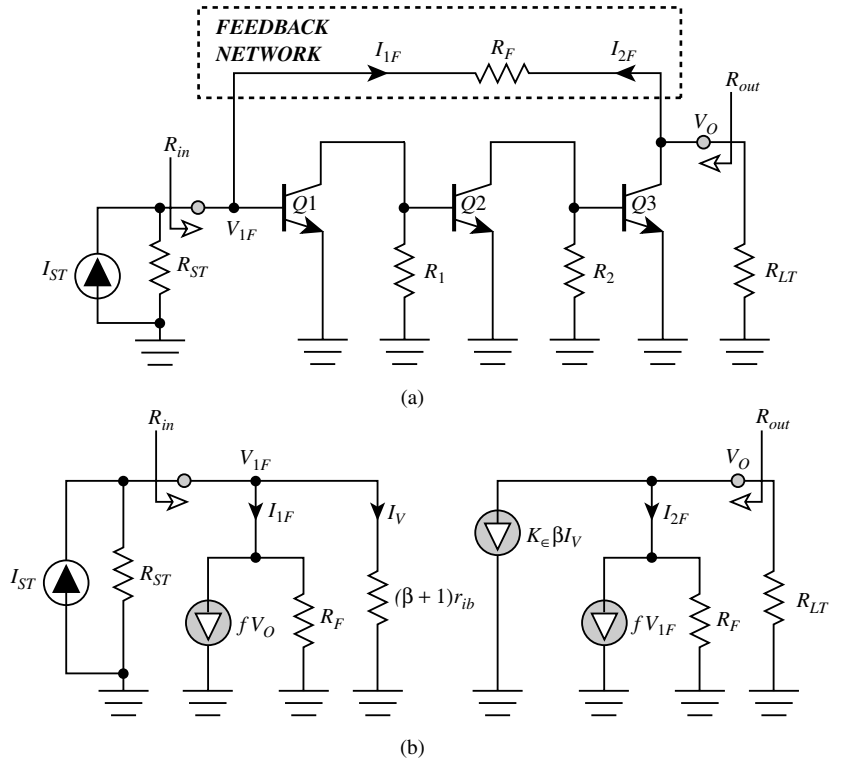

FIGURE 12.8 (a) AC schematic diagram of a bipolar shunt-shunt feedback amplifier. (b) Low-frequency small-signal equivalent circuit of the feedback amplifier.

$$\begin{bmatrix} I_{1F} \\ I_{2F} \end{bmatrix} = \begin{bmatrix} \dfrac{1}{R_F} & -\dfrac{1}{R_F} \\ -\dfrac{1}{R_F} & \dfrac{1}{R_F} \end{bmatrix} \begin{bmatrix} V_{1F} \\ V_O \end{bmatrix} \tag{12.38}$$

which implies that a resistance, R_F, loads both the input and the output ports of the open-loop three-stage cascade. The short-circuit admittance relationship in (12.38) also suggests a feedback factor, f, given by

$$f = \frac{1}{R_F} \tag{12.39}$$

The foregoing observations and the small-signal modeling experience gained with the preceding two feedback amplifiers lead to the equivalent circuit submitted in Figure 12.8(b). For analytical simplicity, the model reflects the assumption that all three transistors in the open loop have identical small-signal parameters. Moreover, the constant, K_ε, which symbolizes the ratio of the signal base current flowing into transistor $Q3$ to the signal base current conducted by transistor $Q1$, is given by

$$K_\in = \left[\frac{\alpha R_1}{r_{ib} + (1-\alpha)R_1}\right]\left[\frac{\alpha R_2}{r_{ib} + (1-\alpha)R_2}\right] \tag{12.40}$$

Finally, the voltage-controlled current source, fV_{1F}, accounts for feed-forward signal transmission through the feedback network. If such feed-forward is to be negligible, the magnitude of this controlled current

must be significantly smaller than $K_\varepsilon \beta I_v$, a current that emulates feed-forward through the open-loop amplifier. Noting that the input port voltage, V_{1F}, in the present case remains the same as that specified by (12.29), negligible feed-forward through the feedback network mandates

$$R_F \gg \frac{r_{ib}}{\alpha K_\varepsilon} \tag{12.41}$$

Because the constant K_ε in (12.40) tends toward β^2 if R_1 and R_2 are large resistances, (12.41) is relatively easy to satisfy.

With feed-forward through the feedback network ignored, an analysis of the model in Figure 12.8(b) provides an open-loop transresistance, $R_{MO}(R_{ST}, R_{LT})$, of

$$R_{MO}\left(R_{ST}, R_{LT}\right) = -\alpha K_\varepsilon \left[\frac{R_F \| R_{ST}}{r_{ib}\left(1-\alpha\right)\left(R_F \| R_{ST}\right)}\right]\left(R_F \| R_{LT}\right) \tag{12.42}$$

while the loop gain is

$$\begin{aligned} T = fR_{MO}\left(R_{ST}, R_{LT}\right) &= -\frac{R_{MO}\left(R_{ST}, R_{LT}\right)}{R_F} \\ &= \alpha K_\varepsilon \left[\frac{R_{ST}}{R_{ST}+R_F}\right]\left[\frac{R_F \| R_{ST}}{r_{ib}\left(1-\alpha\right)\left(R_F \| R_{ST}\right)}\right] \end{aligned} \tag{12.43}$$

For $T \gg 1$, the corresponding closed-loop transresistance $R_M(R_{ST}, R_{LT})$ is

$$R_M\left(R_{ST}, R_{LT}\right) = \frac{R_{MO}\left(R_{ST}, R_{LT}\right)}{1+T} \approx -R_F \tag{12.44}$$

Finally, the approximate driving-point input and output resistances are, respectively,

$$R_{in} \approx \left(\frac{r_{ib}}{\alpha K_\varepsilon}\right)\left(1+\frac{R_F}{R_{LT}}\right) \tag{12.45}$$

$$R_{out} \approx \left[\frac{r_{ib}+\left(1-\alpha\right)\left(R_F \| R_{ST}\right)}{\alpha K_\varepsilon}\right]\left(1+\frac{R_F}{R_{ST}}\right) \tag{12.46}$$

Design Considerations

Because the shunt-shunt triple uses three gain stages in the open-loop amplifier, its loop gain is significantly larger than the loop gains provided by either of the previously considered feedback cells. Accordingly, the feedback triple affords superior desensitization of the closed-loop gain with respect to transistor parameters and source and load resistances; but the presence of a cascade of three common emitter gain stages in the open loop of the amplifier complicates frequency compensation and limits the 3-dB bandwidth. The problem is that, although each common emitter stage approximates a dominant pole amplifier, none of the critical frequencies in the cluster of poles established by the cascade interconnection of these units is likely to be dominant. The uncompensated closed loop is therefore predisposed to unacceptable underdamping, thereby making compensation via an introduced feedback zero difficult.

At least three compensation techniques can be exploited to optimize the performance of the shunt-shunt feedback amplifier [3], [7–9]. The first of these techniques entail pole splitting of the open-loop

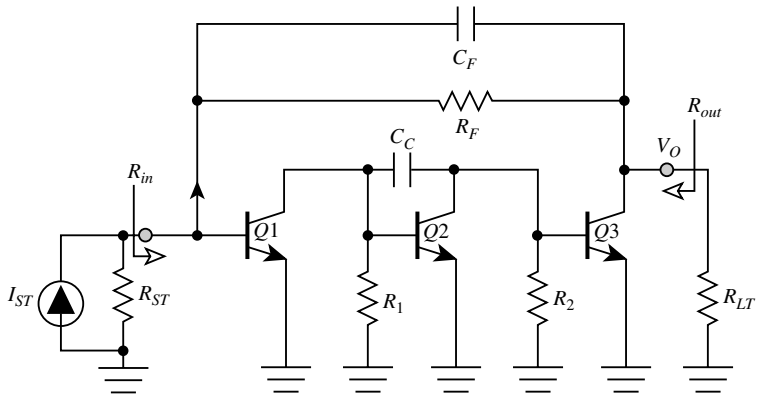

FIGURE 12.9 AC schematic diagram of a frequency compensated shunt-shunt triple. The capacitance, C_c, achieves open-loop pole splitting, while the capacitance, C_F, implements a compensating feedback network zero.

interstage through the introduction of a capacitance, C_c, between the base and the collector terminals of transistor $Q2$, as depicted in the ac schematic diagram of Figure 12.9. In principle, pole splitting can be invoked on any one of the three stages of the open loop; but pole splitting of the interstage is most desirable because such compensation of the first stage proves effective only for large source resistance. Moreover, the resultant dominant pole becomes dependent on the source termination. On the other hand, pole splitting of the third stage produces a dominant pole that is sensitive to load termination. In conjunction with pole splitting, a feedback zero can be introduced, if necessary, to increase closed-loop damping by replacing the feedback resistance, R_F, by the parallel combination of R_F and a feedback capacitance, C_F, as illustrated in Figure 12.9. This compensation produces left-half-plane zero in the feedback factor at $s = -(1/R_F)$.

A second compensation method broadbands the interstage of the open-loop amplifier through local current feedback introduced by the resistance, R_X, in Figure 12.10. Simultaneously, the third stage is broadbanded by way of a common base cascode transistor $Q4$. Because emitter degeneration of the interstage reduces the open-loop gain, an emitter follower (transistor $Q5$) is embedded between the feedback network

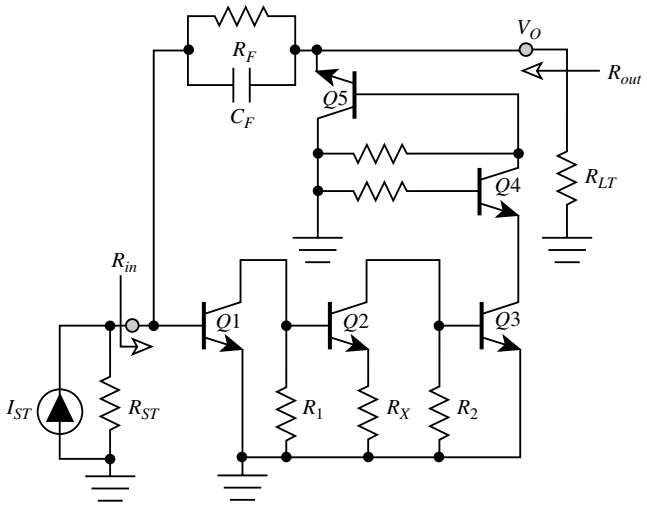

FIGURE 12.10 AC schematic diagram of an alternative compensation scheme for the shunt-shunt triple. Transistor $Q2$ is broadbanded by the emitter degeneration resistance R_X and transistor $Q3$ is broadbanded by the common base cascode transistor $Q4$. The emitter follower transistor, $Q5$, minimizes feed-forward signal transmission through the feedback network.

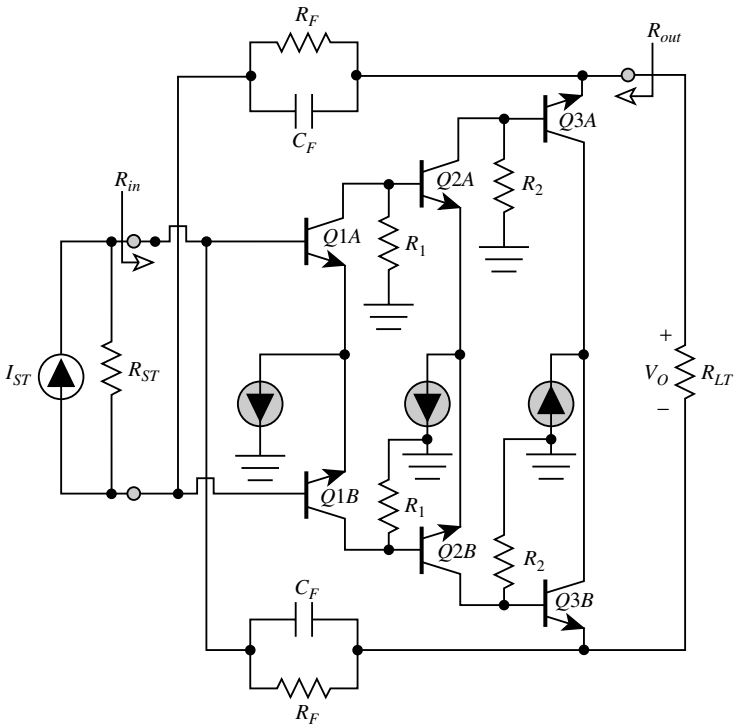

FIGURE 12.11 AC schematic diagram of a differential realization of the compensated shunt-shunt feedback amplifier. The balanced stage boasts improved bandwidth over its single-ended counterpart because of its use of only two high-gain stages in the open loop. The emitter follower pair *Q*3A and *Q*3B diminishes feed-forward transmission through the feedback network composed of the shunt interconnection of resistor R_F with capacitor C_F.

and the output port of the open-loop third stage. As in the case of the series-shunt feedback amplifier, the first-order effect of this emitter follower is to increase feed-forward signal transmission through the open-loop amplifier by a factor that approaches $(\beta + 1)$.

A final compensation method is available if shunt-shunt feedback is implemented as the balanced differential architecture (see the ac schematic diagram offered in Figure 12.11). By exploiting the antiphase nature of opposite collectors in a balanced common emitter topology, a shunt-shunt feedback amplifier can be realized with only two gain stages in the open loop. The resultant closed loop 3-dB bandwidth is invariably larger than that of its three-stage single-ended counterpart, because the open loop is now characterized by only two, as opposed to three, fundamental critical frequencies. Because the forward gain implicit to two amplifier stages is smaller than the gain afforded by three stages of amplification, a balanced emitter follower (transistors *Q*3*A* and *Q*3*B*) is incorporated to circumvent the deleterious relative effects of feed-forward signal transmission through the feedback network.

12.5 Series-Series Feedback Amplifier

Figure 12.12(a) is the ac schematic diagram of the series-series feedback amplifier. Three transistors, *Q*1, *Q*2, and *Q*3, are embedded in the open-loop amplifier, while the feedback subcircuit is the wye configuration formed of the resistances R_X, R_Y, and R_Z. Although it is possible to realize series-series feedback via emitter degeneration of a single-stage amplifier, the series-series triple offers substantially more loop gain and thus better desensitization of the forward gain with respect to both transistor parameters and source and load terminations.

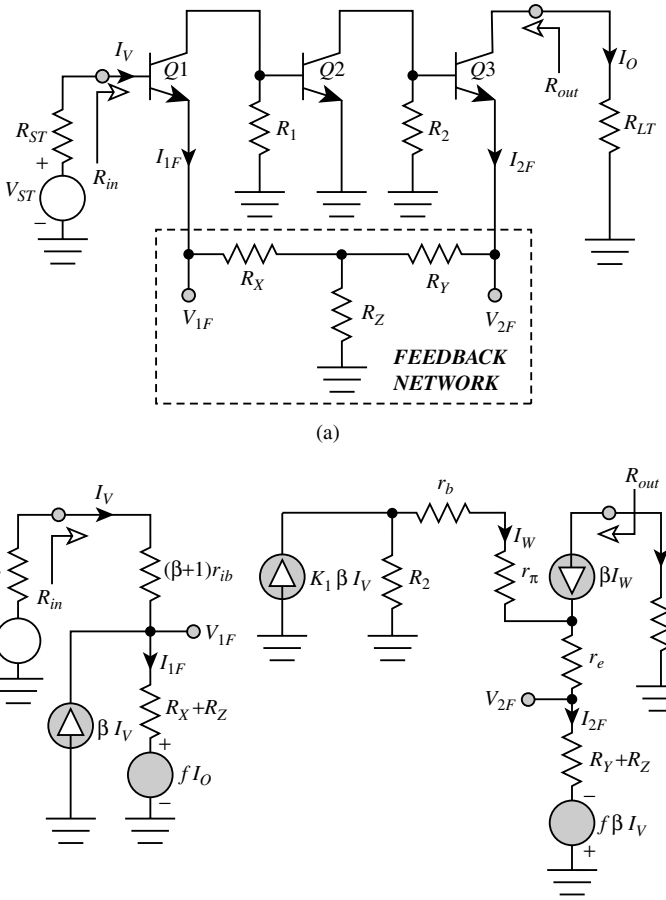

FIGURE 12.12 (a) AC schematic diagram of a bipolar series-series feedback amplifier. (b) Low-frequency, small-signal equivalent circuit of the feedback amplifier.

In Figure 12.12(a), the feedback wye senses the $Q3$ emitter current, which is a factor of $(1/\alpha)$ of the output signal current I_o. This sampled current is fed back as a voltage in series with the emitter of $Q1$. Because output current is fed back as a voltage to a voltage-driven input port, both the driving point input and output resistances are large. The circuit is therefore best suited as a transconductance amplifier in the sense that for large loop gain, its closed-loop transconductance, $G_M(R_{ST}, R_{LT}) = I_O/V_{ST}$, is almost independent of the source and load resistances.

The series-series topology of the subject amplifier conduces z-parameter modeling of the feedback network. Noting the electrical variables delineated in the diagram of Figure 12.12(a),

$$\begin{bmatrix} V_{1F} \\ V_{2F} \end{bmatrix} = \begin{bmatrix} R_X + R_Z & R_Z \\ R_Z & R_Y + R_Z \end{bmatrix} \begin{bmatrix} I_{1F} \\ I_{2F} \end{bmatrix} \tag{12.47}$$

Equation (12.47) suggests that the open-circuit feedback network resistances loading the emitters of transistors $Q1$ and $Q3$ are $(R_X + R_Z)$ and $(R_Y + R_Z)$, respectively, and the voltage fed back to the emitter of transistor $Q1$ is $R_Z I_{2F}$. Because the indicated feedback network current I_{2F} is $(-I_O/\alpha)$, this fed back voltage is equivalent to $(-R_Z I_O/\alpha)$, which suggests a feedback factor, f, of

$$f = \frac{R_Z}{\alpha} \tag{12.48}$$

Finally, the feed-forward through the feedback network if $R_Z I_{1F}$. Because I_{1F} relates to the signal base current I_V flowing into transistor $Q1$ by $I_{1F} = (\beta + 1)I_v$, this feed-forward voltage is also expressible as $(-f\,\beta I_v)$. The foregoing observations and the hybrid-pi method of a bipolar junction transistor produce the small-signal model depicted in Figure 12.12(b). In this model, all transistors are presumed to have identical corresponding small-signal parameters, and the constant, K_1, is

$$K_1 = \frac{\alpha R_1}{r_{ib} + (1-\alpha)R_1} \tag{12.49}$$

An analysis of the model of Figure 12.12(b) confirms that the ratio of the signal current, I_W, flowing into the base of transistor $Q3$ to the signal base current, I_V, of transistor $Q1$ is

$$\frac{I_W}{I_V} = \frac{\alpha K_1 R_2 \left(1 + \dfrac{f}{K_1 R_2}\right)}{r_{ib} + R_Y + R_Z + (1-\alpha)R_2} \tag{12.50}$$

This result suggests that feed-forward effects through the feedback network are negligible if $|f| \ll K_1 R_2$, which requires

$$R_Z \ll \alpha K_1 R_2 \tag{12.51}$$

In view of the fact that the constant, K_1, approaches β for large values of the resistance, R_1, (12.51) is not a troublesome inequality. Introducing a second constant, K_2, such that

$$K_2 \triangleq \frac{\alpha R_2}{r_{ib} + R_Y + R_Z + (1-\alpha)R_2} \tag{12.52}$$

the ratio I_W/I_V in (12.50) becomes

$$\frac{I_W}{I_V} \approx K_1 K_2 \tag{12.53}$$

assuming (12.51) is satisfied.

Given the propriety of (12.50) and using (12.53) the open-loop transconductance, $G_{MO}(R_{ST}, R_{LT})$ is found to be

$$G_{MO}(R_{ST}, R_{LT}) = -\left\{\frac{\alpha K_1 K_2}{r_{ib} + R_X + R_Z + (1-\alpha)R_{ST}}\right\} \tag{12.54}$$

and recalling (12.48), the loop gain T is

$$T = -\left(\frac{R_Z}{\alpha}\right) G_{MO}(R_{ST}, R_{LT}) = \frac{K_1 K_2 R_Z}{r_{ib} + R_X + R_Z + (1-\alpha)R_{ST}} \tag{12.55}$$

It follows that for $T \gg 1$, the closed-loop transconductance is

$$G_M(R_{ST}, R_{LT}) = \frac{G_{MO}(R_{ST}, R_{LT})}{1+T} \approx -\frac{\alpha}{R_Z} \tag{12.56}$$

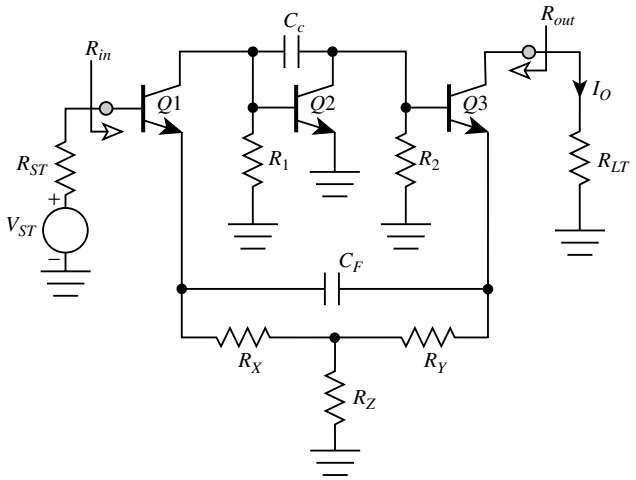

FIGURE 12.13 AC schematic diagram of a frequency compensated series-series feedback triple. The capacitance, C_c, achieves pole splitting in the open-loop configuration, while the capacitance, C_F, introduces a zero in the feedback factor of the closed-loop amplifier.

The Early resistance is large enough to justify its neglect, so the open-loop, and thus the closed-loop, driving-point output resistances are infinitely large. On the other hand, the closed-loop driving point input resistance R_{in} can be shown to be

$$R_{\text{in}} = R_{\text{ino}}\left[1 + f\,G_{\text{MO}}\left(0, R_{\text{LT}}\right)\right] \approx \left(\beta + 1\right)K_1 K_2 R_Z \tag{12.57}$$

Similar to its shunt-shunt counterpart, the series-series feedback amplifier uses three open-loop gain stages to produce large loop gain. However, also similar to the shunt-shunt triple, frequency compensation via an introduced feedback zero is difficult unless design care is exercised to realize a dominant pole open-loop response. To this end, the most commonly used compensation is pole splitting in the open loop, combined, if required, with the introduction of a zero in the feedback factor. The relevant ac schematic diagram appears in Figure 12.13 where the indicated capacitance, C_c, inserted across the base-collector terminals of transistor $Q3$ achieves the aforementioned pole splitting compensation. The capacitance, C_F, in Figure 12.13 delivers a frequency-dependent feedback factor, $f\,(s)$ of

$$f(s) = f\left[\frac{1 + \dfrac{s}{z}}{1 + \dfrac{s}{z}\left(\dfrac{R_Z}{R_Z + R_X \| R_Y}\right)}\right] \tag{12.58}$$

where the frequency z of the introduced zero derives from

$$\frac{1}{z} = \left(R_X + R_Y\right)\left(1 + \frac{R_X \| R_Y}{R_Z}\right)C_F \tag{12.59}$$

The corresponding pole in (12.58) is insignificant if the closed-loop amplifier is designed for a bandwidth, B_{cl} that satisfies the inequality, $B_{\text{cl}}(R_X + R_Y)C_F \ll 1$.

As is the case with shunt-shunt feedback, an alternative frequency compensation scheme is available if series-series feedback is implemented as a balanced differential architecture. The pertinent ac schematic

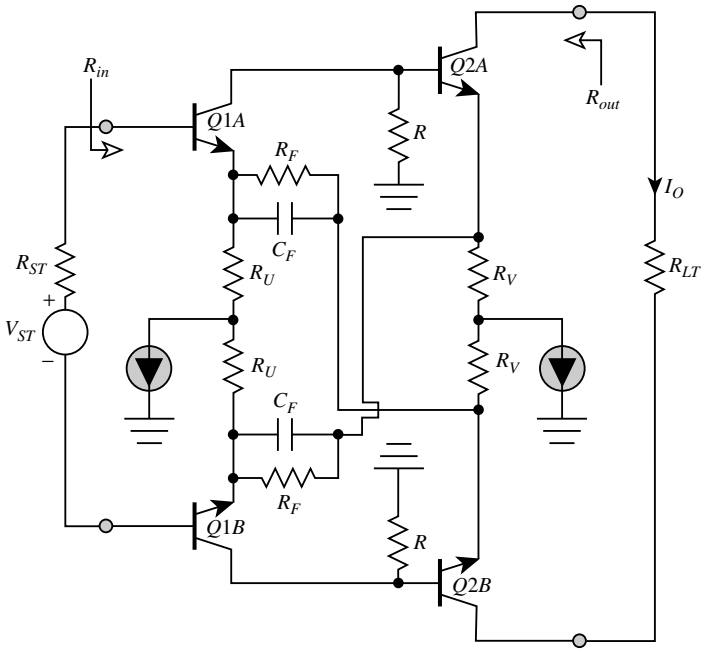

FIGURE 12.14 AC schematic diagram of a balanced differential version of the series-series feedback amplifier. The circuit utilizes only two, as opposed to three, gain stages in the open loop.

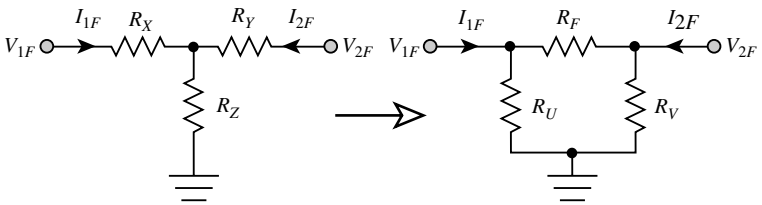

FIGURE 12.15 Transformation of the wye feedback subcircuit used in the amplifier of Figure 12.13 to the delta subcircuit exploited in Figure 12.14. The resistance transformation equations are given by (12.60)–(12.62).

diagram, inclusive of feedback compensation, appears in Figure 12.14. This diagram exploits the fact that the feedback wye consisting of the resistances, R_X, R_Y, and R_Z as utilized in the single-ended configurations of Figures 12.12(a) and 12.13 can be transformed into the feedback delta of Figure 12.15. The terminal volt-ampere characteristics of the two networks in Figure 12.15 are identical, provided that the delta subcircuit elements, R_F, R_U, and R_V, are chosen in accordance with

$$R_F = \left(R_X + R_Y\right)\left(1 + \frac{R_X \| R_Y}{R_Z}\right) \tag{12.60}$$

$$\frac{R_U}{R_F} = \frac{R_Z}{R_Y} \tag{12.61}$$

$$\frac{R_V}{R_F} = \frac{R_Z}{R_X} \tag{12.62}$$

12.6 Dual-Loop Feedback

As mentioned previously, a simultaneous control of the driving point I/O resistances, as well as the closed-loop gain, mandates the use of dual global loops comprised of series and shunt feedback signal paths. The two global dual-loop feedback architectures are the **series-series/shunt-shunt feedback amplifier** and the **series-shunt/shunt-series feedback amplifier**. In the following subsections, both of these units are studied by judiciously applying the relevant analytical results established earlier for pertinent single-loop feedback architectures. The ac schematic diagrams of these respective circuit realizations are provided, and engineering design considerations are offered.

Series-Series/Shunt-Shunt Feedback Amplifier

Figure 12.16 is a behavioral abstraction of the series-series/shunt-shunt feedback amplifier. Two port z parameters are used to model the series-series feedback subcircuit, for which feed-forward is tacitly ignored and the feedback factor associated with its current controlled voltage source is f_{ss}. On the other hand, y parameters model the shunt-shunt feedback network, where the feedback factor relative to its voltage controlled current source is f_{pp}. As in the series-series network, feed-forward in the shunt-shunt subcircuit is presumed negligible. The four-terminal amplifier around which the two feedback units are connected has an open loop (meaning $f_{ss} = 0$ and $f_{pp} = 0$, but with the loading effects of both feedback circuits considered) transconductance of $G_{\mathrm{MO}}(R_{\mathrm{ST}}, R_{\mathrm{LT}})$.

With f_{pp} set to zero to deactivate shunt-shunt feedback, the resultant series-series feedback network is a transconductance amplifier with a closed-loop transconductance, $G_{\mathrm{MS}}(R_{\mathrm{ST}}, R_{\mathrm{LT}})$, is

$$G_{\mathrm{MS}}\left(R_{\mathrm{ST}}, R_{\mathrm{LT}}\right) = \frac{I_O}{V_{\mathrm{ST}}} = \frac{G_{\mathrm{MO}}(R_{\mathrm{ST}}, R_{\mathrm{LT}})}{1 + f_{ss} G_{\mathrm{MO}}\left(R_{\mathrm{ST}}, R_{\mathrm{LT}}\right)} \approx \frac{1}{f_{ss}} \tag{12.63}$$

where the loop gain, $f_{ss}G_{\mathrm{MO}}(R_{\mathrm{ST}}, R_{\mathrm{LT}})$, is presumed much larger than one, and the loading effects of both the series-series feedback subcircuit and the deactivated shunt-shunt feedback network are incorporated

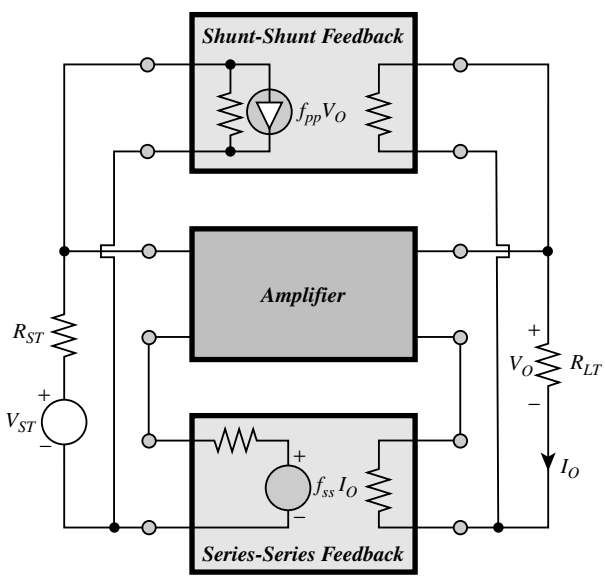

FIGURE 12.16 System-level diagram of a series-series/shunt-shunt dual-loop feedback amplifier. Note that feed-forward signal transmission through either feedback network is ignored.

into $G_{MO}(R_{ST}, R_{LT})$. The transresistance, $R_{MS}(R_{ST}, R_{LT})$, implied by (12.63), which expedites the study of the shunt-shunt component of the feedback configuration, is

$$R_{MS}\left(R_{ST}, R_{LT}\right) = \frac{V_O}{I_{ST}} = R_{ST}R_{LT}\frac{I_O}{V_{ST}} \approx \frac{R_{ST}R_{LT}}{f_{ss}} \tag{12.64}$$

The series-series feedback input and output resistances R_{ins} and R_{outs}, respectively, are large and given by

$$R_{ins} = R_{ino}\left[1 + f_{ss}G_{MO}\left(0, R_{LT}\right)\right] \tag{12.65}$$

and

$$R_{outs} = R_{outo}\left[1 + f_{ss}G_{MO}\left(R_{ST}, 0\right)\right] \tag{12.66}$$

where the zero feedback ($f_{ss} = 0$ and $f_{pp} = 0$) values, R_{ino} and R_{outo}, of these driving point quantities are computed with due consideration given to the loading effects imposed on the amplifier by both feedback subcircuits.

When shunt-shunt feedback is applied around the series-series feedback cell, the configuration becomes a transresistance amplifier. The effective open-loop transresistance is $R_{MS}(R_{ST}, R_{LT})$, as defined by (12.64). Noting a feedback of f_{pp}, the corresponding closed-loop transresistance is

$$R_M\left(R_{ST}, R_{LT}\right) \approx \frac{\dfrac{R_{ST}R_{LT}}{f_{ss}}}{1 + f_{pp}\left(\dfrac{R_{ST}R_{LT}}{f_{ss}}\right)} \tag{12.67}$$

which is independent of amplifier model parameters, despite the unlikely condition of an effective loop gain $f_{pp}R_{ST}R_{LT}/f_{ss}$ that is much larger than one. It should be interjected, however, that (12.67) presumes negligible feed-forward through the shunt-shunt feedback network. This presumption may be inappropriate owing to the relatively low closed-loop gain afforded by the series-series feedback subcircuit. Ignoring this potential problem temporarily, (12.67) suggests a closed-loop voltage gain $A_V\,(R_{ST}, R_{LT})$ of

$$A_V\left(R_{ST}, R_{LT}\right) = \frac{V_O}{V_S} = \frac{R_M\left(R_{ST}, R_{LT}\right)}{R_{ST}} \approx \frac{R_{LT}}{f_{ss} + f_{pp}R_{ST}R_{LT}} \tag{12.68}$$

The closed-loop, driving-point output resistance R_{out}, can be straightforwardly calculated by noting that the open circuit ($R_{LT} \to \infty$) voltage gain, A_{VO}, predicted by (12.68) is $A_{VO} = 1/f_{pp}\,R_{ST}$. Accordingly, (12.68) is alternatively expressible as

$$A_V\left(R_{ST}, R_{LT}\right) \approx A_{VO}\left(\frac{R_{LT}}{R_{LT} + \dfrac{f_{ss}}{f_{pp}R_{ST}}}\right) \tag{12.69}$$

Because (12.69) is a voltage divider relationship stemming from a Thévenin model of the output port of the dual-loop feedback amplifier, as delineated in Figure 12.17, it follows that the driving-point output resistance is

$$R_{out} \approx \frac{f_{ss}}{f_{pp}R_{ST}} \tag{12.70}$$

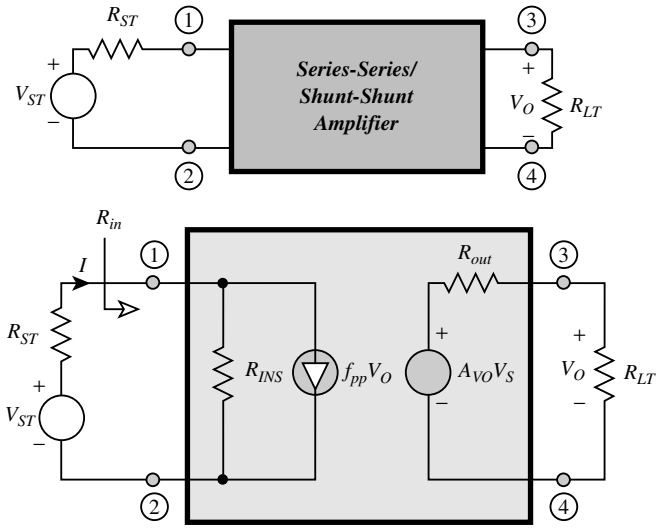

FIGURE 12.17 Norton equivalent input and Thévenin equivalent output circuits for the series-series/shunt-shunt dual-loop feedback amplifier.

Observe that, similar to the forward gain characteristics, the driving-point output resistance is nominally insensitive to changes and other uncertainties in open-loop amplifier parameters. Moreover, this output resistance is directly proportional to the ratio f_{ss}/f_{pp} of feedback factors. As is illustrated in preceding sections, the individual feedback factors, and thus the ratio of feedback factors, is likely to be proportional to a ratio of resistances. In view of the fact that resistance ratios can be tightly controlled in a monolithic fabrication process, R_{out} in (12.70) is accurately prescribed for a given source termination.

The driving-point input resistance R_{in} can be determined from a consideration of the input port component of the system level equivalent circuit depicted in Figure 12.17. This resistance is the ratio of V_{ST} to I, under the condition of $R_S = 0$. With $R_S = 0$, (12.68) yields $V_O = R_{\text{LT}}V_{\text{ST}}/f_{ss}$ and thus, Kirchhoff's voltage law (KVL) applied around the input port of the model at hand yields

$$R_{\text{in}} = \frac{R_{\text{ins}}}{1 + \dfrac{f_{pp}R_{\text{LT}}R_{\text{ins}}}{f_{ss}}} \approx \frac{f_{ss}}{f_{pp}R_{\text{LT}}} \tag{12.71}$$

where the "open-loop" input resistance R_{ins}, defined by (12.65), is presumed large. Similar to the driving-point output resistance of the series-series/shunt-shunt feedback amplifier, the driving-point input resistance is nominally independent of open-loop amplifier parameters.

It is interesting to observe that the input resistance in (12.71) is inversely proportional to the load resistance by the same factor (f_{ss}/f_{pp}) that the driving-point output resistance in (12.70) is inversely proportional to the source resistance. As a result,

$$\frac{f_{ss}}{f_{pp}} \approx R_{\text{in}}R_{\text{LT}} \equiv R_{\text{out}}R_{\text{ST}} \tag{12.72}$$

Thus, in addition to being stable performance indices for well-defined source and load terminations, the driving-point input and output resistances track one another, despite manufacturing uncertainties and changes in operating temperature that might perturb the individual values of the two feedback factors f_{ss} and f_{pp}.

The circuit property stipulated by (12.72) has immediate utility in the design of wideband communication transceivers and other high-speed signal-processing systems [10–14]. In these and related applications, a cascade of several stages is generally required to satisfy frequency response, distortion, and noise specifications. A convenient way of implementing a cascade interconnection is to force each member of the cascade to operate under the match terminated case of $R_{ST} = R_{in} = R_{LT} = R_{out} \triangleq R$. From (12.72) match terminated operation demands feedback factors selected so that

$$R = \sqrt{\frac{f_{ss}}{f_{pp}}} \tag{12.73}$$

which forces a match terminated closed-loop voltage gain A_V^* of

$$A_V^* \approx \frac{1}{2f_{pp}R} = \frac{1}{2\sqrt{f_{pp}f_{ss}}} \tag{12.74}$$

The ac schematic diagram of a practical, single-ended series-series/shunt-shunt amplifier is submitted in Figure 12.18. An inspection of this diagram reveals a topology that coalesces the series-series and shunt-shunt triples studied earlier. In particular, the wye network formed of the three resistances, R_{Xx}, R_Y, and R_Z, comprises the series-series component of the dual-loop feedback amplifier. The capacitor, C_c, narrowbands the open-loop amplifier to facilitate frequency compensation of the series-series loop through the capacitance, C_{F1}. Compensated shunt feedback of the network is achieved by the parallel combination of the resistance, R_F and the capacitance, C_{F2}. If C_{F1} and C_c combine to deliver a dominant pole series-series feedback amplifier, C_{F2} is not necessary. Conversely, C_{F1} is superfluous if C_{F2} and C_c interact to provide a dominant pole shunt-shunt feedback amplifier. As in the single ended series-series configuration, transistor $Q3$ can be broadbanded via a common base cascode. Moreover, if feedback through the feedback networks poses a problem, an emitter follower can be inserted at the port to which the shunt feedback path and the load termination are incident.

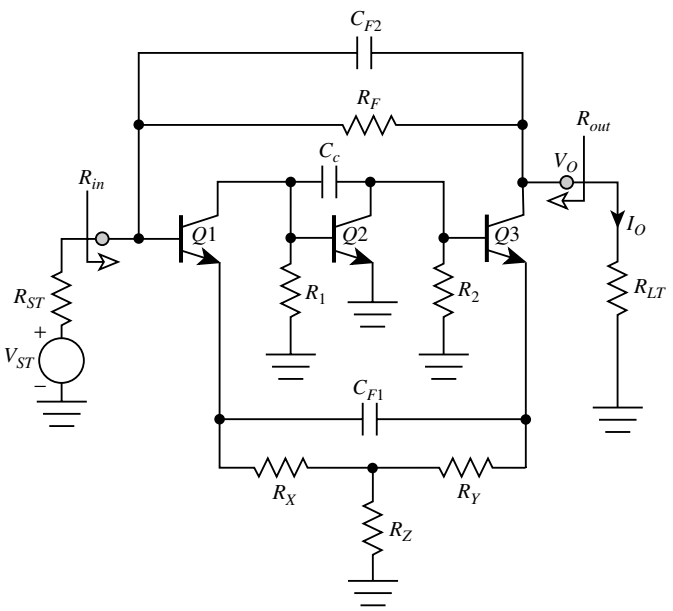

FIGURE 12.18 AC schematic diagram of a frequency-compensated, series-series/shunt-shunt, dual-loop feedback amplifier. The compensation is affected by the capacitances C_{F1} and C_{F2}, while C_c achieves pole splitting in the open-loop amplifier.

A low-frequency analysis of the circuit in Figure 12.18 is expedited by assuming high beta transistors having identical corresponding small-signal model parameters. This analysis, which in contrast to the simplified behavioral analysis, does not ignore the electrical effects of the aforementioned feed-forward through the shunt-shunt feedback network, yields a voltage gain $A_V\,(R_{ST}, R_{LT})$, of

$$A_V\left(R_{ST}, R_{LT}\right) \approx -\left(\frac{R_{in}}{R_{in}+R_{ST}}\right)\left(\frac{R_{LT}}{R_{LT}+R_F}\right)\left(\frac{\alpha R_F}{R_Z}-1\right) \tag{12.75}$$

where the driving-point input resistance of the amplifier R_{in} is

$$R_{in} \approx \frac{R_F + R_{LT}}{1+\dfrac{\alpha R_{LT}}{R_Z}} \tag{12.76}$$

The driving-point output resistance R_{out} is

$$R_{out} \approx \frac{R_F + R_{ST}}{1+\dfrac{\alpha R_{ST}}{R_z}} \tag{12.77}$$

As predicted by the behavioral analysis R_{in}, R_{out}, and $A_V\,(R_{ST}, R_{LT})$, are nominally independent of transistor parameters. Observe that the functional dependence of R_{in} on the load resistance, R_{LT}, is identical to the manner in which R_{out} is related to the source resistance R_{ST}. In particular, $R_{in} \equiv R_{out}$ if $R_{ST} \equiv R_{LT}$. For the match terminated case in which $R_{ST} = R_{in} = R_{LT} = R_{out} \triangleq R$,

$$R \approx \sqrt{\frac{R_F R_Z}{\alpha}} \tag{12.78}$$

The corresponding match terminated voltage gain in (12.75) collapses to

$$A_V^* \approx -\left(\frac{R_F - R}{2R}\right) \tag{12.79}$$

Similar to the series-series and shunt-shunt triples, many of the frequency compensation problems implicit to the presence of three open-loop stages can be circumvented by realizing the series-series/shunt-shunt amplifier as a two-stage differential configuration. Figure 12.19 is the acschematic diagram of a compensated differential series-series/shunt-shunt feedback dual.

Series-Shunt/Shunt-Series Feedback Amplifier

The only other type of global dual loop architecture is the series-shunt/shunt-series feedback amplifier; the behavioral diagram appears in Figure 12.20. The series-shunt component of this system, which is modeled by *h*-parameters, has a negligibly small feed-forward factor and a feedback factor of f_{sp}. Hybrid *g*-parameters model the shunt-series feedback structure, which has a feedback factor of f_{ps} and a presumably negligible feed-forward factor. The four-terminal amplifier around which the two feedback units are connected has an open-loop (meaning $f_{sp} = 0$ and $f_{ps} = 0$, but with the loading effects of both feedback circuits considered) voltage gain of $A_{VO}(R_{ST}, R_{LT})$.

For $f_{ps} = 0$, the series-shunt feedback circuit voltage gain $A_{VS}(R_{ST}, R_{LT})$, is

$$A_{VS}\left(R_{ST}, R_{LT}\right) = \frac{V_O}{V_{ST}} = \frac{A_{VO}\left(R_{ST}, R_{LT}\right)}{1+f_{sp}A_{VO}\left(R_{ST}, R_{LT}\right)} \approx \frac{1}{f_{sp}} \tag{12.80}$$

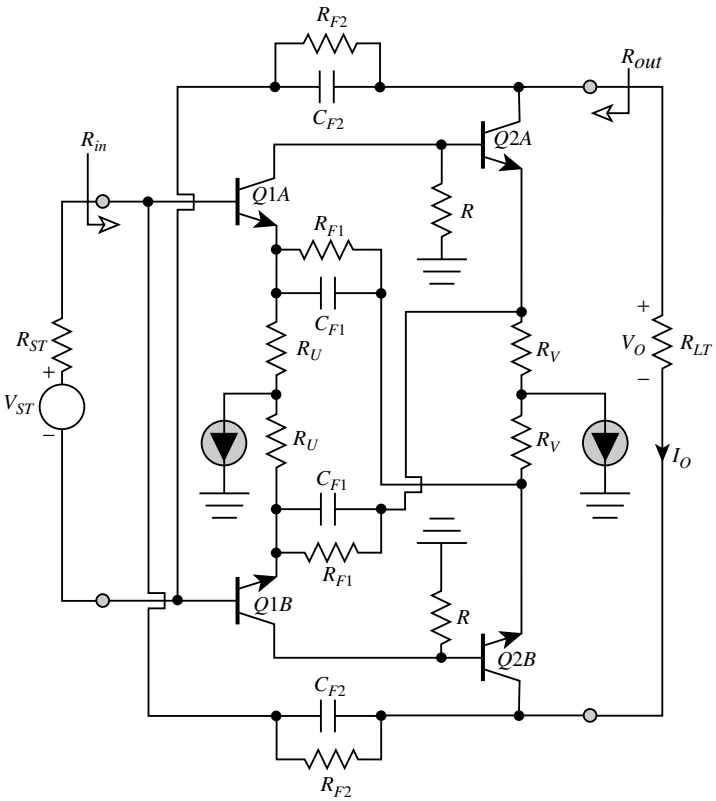

FIGURE 12.19 AC schematic diagram of the differential realization of a compensated series-series/shunt-shunt feedback amplifier.

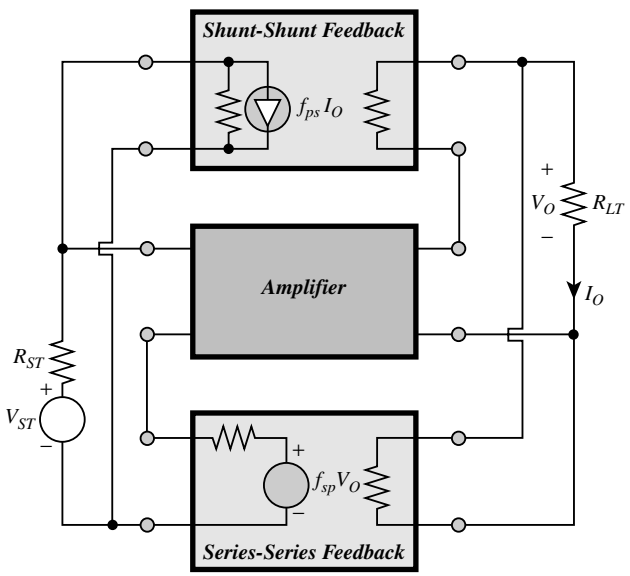

FIGURE 12.20 System level diagram of a series-shunt/shunt-series, dual-loop feedback amplifier. Note that feedforward signal transmission through either feedback network is ignored.

where the approximation reflects an assumption of a large loop gain. When the shunt-series component of the feedback amplifier is activated, the dual-loop configuration functions as a current amplifier. Its effective open-loop transfer function is the current gain, $A_{IS}(R_{ST}, R_{LT})$, established by the series-shunt amplifier; namely,

$$A_{IS}\left(R_{ST}, R_{LT}\right) = \frac{I_O}{I_{ST}} = \left(\frac{R_{ST}}{R_{LT}}\right)\frac{V_O}{V_{ST}} \approx \frac{R_{ST}}{f_{sp}R_{LT}} \tag{12.81}$$

It follows that the current gain, $A_I(R_{ST}, R_{LT})$, of the closed loop is

$$A_I\left(R_{ST}, R_{LT}\right) \approx \frac{\dfrac{R_{ST}}{f_{sp}R_{LT}}}{1 + f_{ps}\left(\dfrac{R_{ST}}{f_{sp}R_{LT}}\right)} = \frac{R_{ST}}{f_{sp}R_{LT} + f_{ps}R_{ST}} \tag{12.82}$$

while the corresponding voltage gain, $A_V(R_{ST}, R_{LT})$, assuming negligible feed-forward through the shunt-series feedback network, is

$$A_V\left(R_{ST}, R_{LT}\right) = \frac{R_{LT}}{R_{ST}} A_I\left(R_{ST}, R_{LT}\right) \approx \frac{R_{LT}}{f_{sp}R_{LT} + f_{ps}R_{ST}} \tag{12.83}$$

Repeating the analytical strategy employed to determine the input and output resistances of the series-series/shunt-shunt configuration, (12.83) delivers a driving-point input resistance of

$$R_{in} \approx \frac{f_{sp}R_{LT}}{f_{ps}} \tag{12.84}$$

and a driving-point output resistance of

$$R_{out} \approx \frac{f_{ps}R_{ST}}{f_{sp}} \tag{12.85}$$

Similar to the forward voltage gain, the driving-point input and output resistances of the series-shunt/shunt-series feedback amplifier are nominally independent of active element parameters. Note, however, that the input resistance is directly proportional to the load resistance by a factor (f_{sp}/f_{ps}), which is the inverse of the proportionality constant that links the output resistance to the source resistance. Specifically,

$$\frac{f_{sp}}{f_{ps}} = \frac{R_{in}}{R_{LT}} = \frac{R_{ST}}{R_{out}} \tag{12.86}$$

Thus, although R_{in} and R_{out} are reliably determined for well-defined load and source terminations, they do not track one another as well as they do in the series-series/shunt-shunt amplifier. Using (12.86), the voltage gain in (12.83) is expressible as

$$A_V\left(R_{ST}, R_{LT}\right) \approx \frac{1}{f_{sp}\left(1 + \sqrt{\dfrac{R_{out}R_{ST}}{R_{in}R_{LT}}}\right)} \tag{12.87}$$

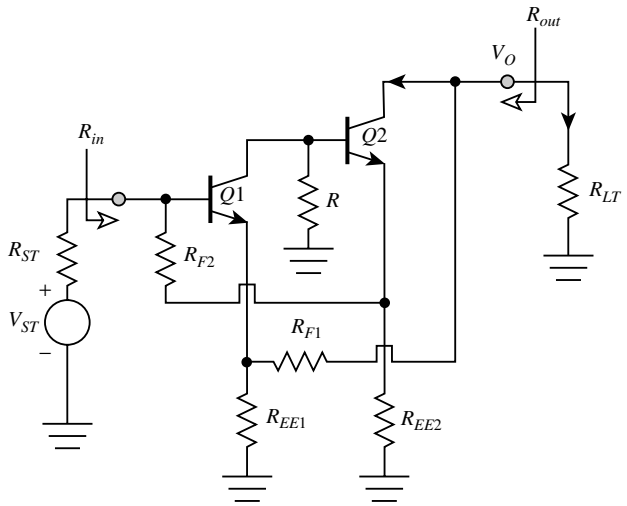

FIGURE 12.21 AC schematic diagram of a series-shunt/shunt-series, dual-loop feedback amplifier.

The simplified ac schematic diagram of a practical series-shunt/shunt-series feedback amplifier appears in Figure 12.21. In this circuit, series-shunt feedback derives from the resistances, R_{EE1} and R_{F1}, and shunt-series feedback is determined by the resistances, R_{EE2} and R_{F2}. Because this circuit topology merges the series-shunt and shunt-series pairs, requisite frequency compensation, which is not shown in the subject figure, mirrors the relevant compensation schemes studied earlier. Note, however, that a cascade of only two open-loop gain stages renders compensation easier to implement and larger 3-dB bandwidths easier to achieve in the series-series/shunt-shunt circuit, which requires three open-loop gain stages for a single-ended application.

For high beta transistors having identical corresponding small-signal model parameters, a low-frequency analysis of the circuit in Figure 12.21 gives a voltage gain of

$$A_V\left(R_{\text{ST}}, R_{\text{LT}}\right) \approx \left(\frac{\alpha R_{\text{in}}}{R_{\text{in}} + \alpha R_S}\right)\left(1 + \frac{R_{\text{F1}}}{R_{\text{EE1}}}\right) \tag{12.88}$$

where the driving-point input resistance, R_{in}, of the subject amplifier is

$$R_{\text{in}} \approx \alpha R_{\text{LT}}\left(\frac{1 + \dfrac{R_{\text{F2}}}{R_{\text{EE2}}}}{1 + \dfrac{R_{\text{F1}}}{R_{\text{EE1}}} + \dfrac{R_{\text{LT}}}{R_{\text{EE1}} \| R_{\text{EE2}}}}\right) \tag{12.89}$$

The driving-point output resistance, R_{out}, is

$$R_{\text{out}} \approx R_{\text{ST}}\left(\frac{1 + \dfrac{R_{\text{F1}}}{R_{\text{EE1}}}}{1 + \dfrac{R_{\text{F2}}}{R_{\text{EE2}}} + \dfrac{R_{\text{ST}}}{R_{\text{EE1}} \| R_{\text{EE2}}}}\right) \tag{12.90}$$

12.7 Summary

This section documents small-signal performance equations, general operating characteristics, and engineering design guidelines for the six most commonly used global feedback circuits. These observations derive from analyses based on the judicious application of signal flow theory to the small-signal model that results when the subject feedback network is supplanted by an appropriate two-port parameter equivalent circuit.

Four of the six fundamental feedback circuits are single-loop architectures.

1. The series-shunt feedback amplifier functions best as a voltage amplifier in that its input resistance is large, and its output resistance is small. Because only two gain stages are required in the open loop, the amplifier is relatively easy to compensate for acceptable closed-loop damping and features potentially large 3-dB bandwidth. A computationally efficient analysis aimed toward determining loop gain, closed-loop gain, I/O resistances, and the condition that renders feed-forward through the feedback network inconsequential is predicated on replacing the feedback subcircuit with its *h*-parameter model.
2. The shunt-series feedback amplifier is a current amplifier in that its input resistance is small, and its output resistance is large. Similar to its series-shunt dual, only two gain stages are required in the open loop. Computationally efficient analyses are conducted by replacing the feedback subcircuit with its *g*-parameter model.
3. The shunt-shunt feedback amplifier is a transresistance signal processor in that both its input and output resistances are small. Although this amplifier can be realized theoretically with only a single open-loop stage, a sufficiently large loop gain generally requires a cascade of three open-loop stages. As a result, pole splitting is invariably required to ensure an open-loop dominant pole response, thereby limiting the achievable closed-loop bandwidth. In addition compensation of the feedback loop may be required for acceptable closed-loop damping. The bandwidth and stability problems implicit to the use of three open-loop gain stages can be circumvented by a balanced differential realization, which requires a cascade of only two open-loop gain stages. Computationally efficient analyses are conducted by replacing the feedback subcircuit with its *y*-parameter model.
4. The series-series feedback amplifier is a transconductance signal processor in that both its input and output resistances are large. Similar to its shunt-shunt counterpart, its implementation generally requires a cascade of three open-loop gain stages. Computationally efficient analyses are conducted by replacing the feedback subcircuit with its *z*-parameter model.

The two remaining feedback circuits are dual-loop topologies that can stabilize the driving-point input and output resistances, as well as the forward gain characteristics, with respect to shifts in active element parameters. One of these latter architectures, the series-series/shunt-shunt feedback amplifier, is particularly well suited to electronic applications that require a multistage cascade.

1. The series-series/shunt-shunt feedback amplifier coalesces the series-series architecture with its shunt-shunt dual. It is particularly well suited to applications, such as wideband communication networks, which require match terminated source and load resistances. Requisite frequency compensation and broadbanding criteria mirror those incorporated in the series-series and shunt-shunt single-loop feedback topologies.
2. The series-shunt/shunt-series feedback amplifier coalesces the series-shunt architecture with its shunt-series dual. Although its input resistance can be designed to match the source resistance seen by the input port of the amplifier, and its output resistance can be matched to the load resistance driven by the amplifier, match terminated operating ($R_{in} = R_{ST} = R_{LT} = R_{out}$) is not feasible. Requisite frequency compensation and broadbanding criteria mirror those incorporated in the series-shunt and shunt-series single-loop feedback topologies.

References

[1] J. Millman and A. Grabel, *Microelectronics,* 2nd ed., New York: McGraw-Hill, 1987, chap. 12.
[2] A. B. Grebene, *Bipolar and MOS Analog Integrated Circuit Design*, New York: Wiley-Interscience, 1984, pp. 424–432.
[3] R. G. Meyer, R. Eschenbach, and R. Chin, "A wideband ultralinear amplifier from DC to 300 MHz," *IEEE J. Solid-State Circuits*, vol. SC-9, pp. 167–175, Aug. 1974.
[4] A. S. Sedra and K. C. Smith, *Microelectronic Circuits*, New York: Holt, Rinehart Winston, 1987, pp. 428–441.
[5] J. M. Early, "Effects of space-charge layer widening in junction transistors," *Proc. IRE*, vol. 46, pp. 1141–1152, Nov. 1952.
[6] A. J. Cote Jr. and J. B. Oakes, *Linear Vacuum-Tube And Transistor Circuits*, New York: McGraw-Hill, 1961, pp. 40–46.
[7] R. G. Meyer and R. A. Blauschild, "A four-terminal wideband monolithic amplifier," *IEEE J. Solid-State Circuits*, vol. SC-17, pp. 634–638, Dec. 1981.
[8] M. Ohara, Y. Akazawa, N. Ishihara, and S. Konaka, "Bipolar monolithic amplifiers for a gigabit optical repeater," *IEEE J. Solid-State Circuits*, vol. SC-19, pp. 491–497, Aug. 1985.
[9] M. J. N. Sibley, R. T. Univin, D. R. Smith, B. A. Boxall, and R. J. Hawkins, "A monolithic transimpedance preamplifier for high speed optical receivers," *British Telecommunicat. Tech. J.*, vol. 2, pp. 64–66, July 1984.
[10] J. F. Kukielka and C. P. Snapp, "Wideband monolithic cascadable feedback amplifiers using silicon bipolar technology," *IEEE Microwave Millimeter-Wave Circuits Symp. Dig.*, vol. 2, pp. 330, 331, June 1982.
[11] R. G. Meyer, M. J. Shensa, and R. Eschenbach, "Cross modulation and intermodulation in amplifiers at high frequencies," *IEEE J. Solid-State Circuits*, vol. SC-7, pp. 16–23, Feb. 1972.
[12] K. H. Chan and R. G. Meyer, "A low distortion monolithic wide-band amplifier," *IEEE J. Solid-State Circuits*, vol. SC-12, pp. 685–690, Dec. 1977.
[13] A. Arbel, "Multistage transistorized current modules," *IEEE Trans. Circuits Syst.*, vol. CT-13, pp. 302–310, Sep. 1966.
[14] A. Arbel, *Analog Signal Processing and Instrumentation*, London: Cambridge University, 1980, chap. 3.
[15] W. G. Beall, "New feedback techniques for high performance monolithic wideband amplifiers," Electron. Res. Group, University of Southern California, Tech. Memo., Jan. 1990.